

1 **The prognostic effects of somatic mutations in ER-positive breast cancer**
2

3 **Authors:**

4 Obi L Griffith, PhD^{1,2,3,4,*}, Nicholas C Spies, BSc^{1,*}, Meenakshi Anurag, PhD^{5,6*}, Malachi Griffith,
5 PhD^{1,2,3,4}, Jingqin Luo, PhD^{3,6}, Dongsheng Tu, PhD⁸, Belinda Yeo, PhD⁹, Jason Kunisaki, BSc¹,
6 Christopher A Miller, PhD^{1,2}, Kilannin Krysiak, PhD^{1,2}, Jasreet Hundal, MSc¹, Benjamin J
7 Ainscough, BSc¹, Zachary L Skidmore, MEng¹, Katie Campbell, BSc¹, Runjun Kumar, BSc²,
8 Catrina Fronick, BSc¹, Lisa Cook, BSc¹, Jacqueline E Snider, BSc², Sherri Davies, PhD², Shyam
9 M Kavuri, PhD^{5,6}, Eric C Chang, PhD^{5,6}, Vincent Magrini, PhD^{1,4,10}, David E Larson, PhD¹,
10 Robert S Fulton, MSc^{1,4}, Shuzhen Liu, MSc⁸, Samuel Leung, MSc⁸, David Voduc, MD⁸, Ron
11 Bose, MD, PhD², Mitch Dowsett PhD, FMedSci⁹, Richard K Wilson, PhD^{1,3,4}, Torsten O Nielsen,
12 MD, PhD⁸, Elaine R Mardis, PhD^{1,3,4,10,†}, Matthew J Ellis MB, BChir, PhD^{5,6†}

13 **Affiliations:**

- 1 1. McDonnell Genome Institute, Washington University School of Medicine, St. Louis, MO
- 2 2. Department of Medicine, Division of Oncology, Washington University School of
Medicine, St. Louis, MO
- 3 3. Siteman Cancer Center, Washington University School of Medicine, St. Louis, MO
- 4 4. Department of Genetics, Washington University School of Medicine, St. Louis, MO
- 5 5. Lester and Sue Smith Breast Center and Dan L. Duncan Cancer Center, Baylor College
of Medicine, Houston, TX
- 6 6. Department of Medicine, Baylor College of Medicine, Houston, TX
- 7 7. Division of Biostatistics, Washington University School of Medicine, St. Louis MO
- 8 8. Genetic Pathology Evaluation Centre, University of British Columbia, Vancouver,
Canada
- 9 9. Institute of Cancer Research, London, UK
- 10 10. Current address: Nationwide Children's Hospital and Department of Pediatrics, The Ohio
State University College of Medicine, Columbus, OH

29 * These authors contributed equally.

30 † Corresponding authors. mjellis@bcm.edu, elaine.mardis@nationwidechildrens.org

34 **Author emails:**

35 obigriffith@wustl.edu, nspies@wustl.edu, anurag@bcm.edu, mgriffit@wustl.edu,
36 jingqinluo@wustl.edu, dtu@ctg.queensu.ca, belinda.yeo@onjcri.org.au, kunisakijh@wustl.edu,
37 c.a.miller@wustl.edu, kkrysiak@wustl.edu, jhundal@wustl.edu, b.ainscough@wustl.edu,
38 zskidmor@wustl.edu, katiecampbell@wustl.edu, runjunkumar@wustl.edu, cfronick@wustl.edu,
39 cooklisa@wustl.edu, jsnider@dom.wustl.edu, sdavies@dom.wustl.edu,
40 meghashyam.kavuri@bcm.edu, echang1@bcm.edu, vincent.magrini@nationwidechildrens.org,
41 delarson@wustl.edu, rfulton22@wustl.edu, shuzhensuzanne.liu@vch.ca,
42 samuel.leung@vch.ca, dvoduc@bccancer.bc.ca, rbose@dom.wustl.edu,
43 mitchell.dowsett@icr.ac.uk, richard.wilson@nationwidechildrens.org, torsten@mail.ubc.ca,
44 elaine.mardis@nationwidechildrens.org, matthew.ellis@bcm.edu

45
46
47
48
49
50
51

52 Abstract

53

54 More than 50 genes are recurrently affected by somatic mutation in estrogen receptor positive
55 (ER+) breast cancer but prognostic effects have not been definitively established. Primary tumor
56 DNA was therefore subjected to targeted sequencing from 625 postmenopausal (UBC-TAM
57 series) and 328 premenopausal (MA12 trial) hormone receptor-positive (HR+) patients.
58 Independent validation of prognostic interactions was achieved using independent data from the
59 METABRIC study. Associations between MAP3K1 and PIK3CA with luminal A status and TP53
60 mutations with Luminal B/non-luminal tumors were observed, validating the methodological
61 approach. In UBC-TAM, *NF1* frame-shift nonsense (FS/NS) mutation was validated as a poor
62 outcome driver. For MA12, poor outcome associated with PIK3R1 mutation was similarly
63 validated. DDR1 mutations were strongly associated with poor prognosis in UBC-TAM despite
64 stringent false-discovery correction ($q=0.0003$). In conclusion, uncommon recurrent somatic
65 mutations should be further explored to create a more complete explanation of the highly
66 variable outcomes that typify ER+ breast cancer.

67

68 Introduction

69

70 While recent genomic studies have provided a comprehensive catalog of genes that accumulate
71 somatic point mutations and small insertions/deletions (indels) in estrogen receptor-positive
72 (ER+) breast cancer, there remains considerable uncertainty as to how these newly discovered
73 mutations relate to disease outcomes¹⁻³. Most genomic discovery cohorts were neither uniformly
74 treated nor followed long enough. For ER+ disease in particular, prognostic studies require
75 prolonged observation since late relapses can occur⁴. Uniform treatment was a feature of a
76 whole genome sequencing study of samples accrued from a neoadjuvant aromatase inhibitor
77 (AI) clinical trial for ER+ clinical stage 2 or 3 disease, although only short-term anti-proliferative
78 response to AI was reported. This investigation identified that mutations in *MAP3K1*, a tumor
79 suppressor gene involved in stress kinase activation, were associated with indolent biological
80 features and low proliferation rates⁵. The resulting hypothesis was that *MAP3K1* mutation would
81 be associated with favorable outcomes. In contrast, *TP53* mutations associated with poor
82 prognosis features and high proliferation rates.

83

84 To more comprehensively address the relationships between somatic mutations and outcomes
85 in ER+ breast cancer, we developed an approach to detect somatic mutations in DNA isolated
86 from formalin fixed tumor blocks that were over 20 years old. After curating existing mutational
87 data from breast cancer genomics discovery studies (Supplementary Data 1), 83 genes were
88 chosen for analysis (Supplementary Table 1). We applied DNA hybrid capture, sequencing and
89 somatic analysis to three ER+ breast cancer discovery cohorts with contrasting clinical
90 characteristics: An older cohort treated with adjuvant tamoxifen and no chemotherapy, a
91 premenopausal cohort uniformly treated with chemotherapy and randomized to tamoxifen
92 versus observation; and a third mixed cohort that was used to expand the mutational landscape
93 analysis (Supplementary Table 2). An analytical pipeline was developed to identify somatic
94 variants while compensating for the lack of matched normal DNA, which is generally unavailable
95 in the setting of older formalin-fixed tumor material. Somatic mutations were analyzed for
96 association with standard clinical variables, wherein mutated *TP53* and *MAP3K1* served as a
97 *priori* hypotheses for poor and good outcome, respectively. Additional objectives were to identify
98 new mutational hotspots and to determine mutation frequencies for therapeutic targets.
99 Validation was possible by comparing our results to those in cBioPortal where the mutational
100 analysis in the METABRIC cohort overlapped with the 83 genes investigated in the study
101 described here.

102

103 Results

104

105 Sequencing and final study cohorts

106

107 University of British Columbia Tamoxifen Series (UBC-TAM): These cases were drawn from a
108 well-annotated cohort of patients treated with adjuvant tamoxifen without chemotherapy⁶. A
109 total of 625 of 632 (98.8%) patient samples that fully met study criteria passed a minimum
110 sequencing quality cutoff of at least 80% of targeted bases covered at greater than 20X (mean
111 coverage: 133X) with other quality metrics described in the supplementary data (Supplementary
112 Figure 1-5 and Supplementary Data 2). The final patient population had an average age of 67 at
113 diagnosis (range: 40-89+). All were treated with five years of adjuvant tamoxifen, and were
114 primarily postmenopausal, grade 2 or 3 cancers, of ductal histologic subtype (Supplementary
115 Table 2). All were ER+ and at least 88.6% were clinically HER2- (13/625 unknown). A subset of
116 463 of these patients had PAM50 subtyping data available from a previous study⁶. The median
117 follow up in the cohort examined was 25 years and one month.

118

119 POLAR cohort: This patient series was a case-control study of ER+ breast tumors, 175 of 194
120 (90.2%) patient samples passed minimum sequencing quality thresholds. A case was defined
121 as any patient who relapsed during follow-up, and controls were defined as lacking relapse
122 through a similar follow-up duration. Based on these definitions, there were 91 cases and 84
123 controls. Of the cases, 43 were early relapses (<5 years since diagnosis) and 48 were late
124 relapses (>5 years). Patients were only included if they received adjuvant endocrine therapy,
125 but chemotherapy was not an exclusion criterion, nor was menopausal status. These cases
126 were used in the mutation landscape and hotspot analyses only.

127

128 NCIC-MA12 Trial cohort. These cases were drawn from a clinical trial in premenopausal
129 women treated with a standard adjuvant chemotherapy regimen and randomized to tamoxifen
130 versus observation. A total of 459 patient samples passed the minimum sequencing quality
131 threshold, of which 328 were hormone receptor positive (HR+), and only the HR+ cohort are
132 included here for most analyses. The majority were premenopausal (mean age of 45). All
133 patients received chemotherapy, and 48% were treated with 5 years of adjuvant tamoxifen. A
134 subset of 255 of these patients had PAM50 subtyping data available. The median follow up in
135 the cohort examined was 9.7 years

136

137 Across the three cohorts, there were 1,259 patient samples that passed minimum sequencing
138 quality thresholds and 1,128 of these were ER+ (UBC-TAM and POLAR) or HR+ (MA12).

139

140 Variant calling and filtering

141

142 A total of over 62 million variants were called in UBC-TAM. After extensive filtering against a set
143 of nearly 70,000 unmatched normal samples and manual review to eliminate common
144 polymorphisms and false positives (see methods), 1,991 putative somatic variants were
145 identified (0 to 26 variants per patient). A set of 1,693 mutations was defined as the “non-silent”
146 set for further analysis that excluded sequencing variants in splice regions, RNA genes (except
147 *MALAT1*), UTRs, introns, and all silent mutations. Finally, a set of 408 frameshift or nonsense
148 mutations was defined. The same filtering method was applied to both the POLAR and MA12
149 datasets. A total of 540 putative somatic mutations (436 non-silent, 145 FS/NS) were identified
150 in POLAR, and 2,104 (1,753 non-silent, 610 FS/NS) in MA12. Full details on these variants are
151 included in Supplementary Data 3 and summarized for key genes in Supplementary Figure 6.

152

153

154

155

156 Mutation landscape analysis.

157 In 1128 samples passing quality control standards, considering only non-silent mutations, 17
158 genes were mutated at a rate greater than 5%, and 6 at a rate greater than 10%; *PIK3CA* was
159 the only gene mutated in greater than 20% of samples (**Figure 1A**). The order from most
160 recurrent to least for the 10 most frequently mutated genes was: *PIK3CA* (41.1%), *TP53*
161 (15.5%), *MLL3* (13.4%), *MAP3K1* (12.0%), *CDH1* (10.5%), *MALAT1* (10.0%), *GATA3* (9.1%),
162 *MLL2* (8.7%), *ARID1A* (7.2%), and *BRCA2* (6.6%). This list correlates well with previously
163 reported recurrently mutated genes. For example, the top 4 most significantly mutated genes in
164 the ER+ subset of TCGA breast project³ were *PIK3CA* (24.3%), *TP53* (14.6%), *GATA3* (8.9%)
165 and *MAP3K1* (6.2%). The overall average mutation rate was estimated as 3.3 per MB of coding
166 sequence (range: 0.5 to 13.8 mutations per MB, excluding samples with no mutations called). In
167 order to determine whether mutations in any gene pair were mutually exclusive or co-occurring in
168 this dataset, a pairwise Chi-squared or Fisher's exact test was performed. Mutations in *PIK3CA*
169 and *MAP3K1* were significantly more likely to co-occur (after BH FDR correction) in TAM
170 dataset, and were near significance in MA12 although not after correction ($p = 0.08$). These
171 results are summarized in Supplementary Data 4.

172

173 Hotspot analysis

174

175 As anticipated⁷, mutations in *PIK3CA* at *E542K*, *E545K*, and *H1047R* were highly recurrent in
176 this study with 69/1259 (5.5%) *E542K*, 104 (8.3%) *E545K*, and 181 (14.4%) *H1047R* mutations
177 (Supplementary Figure 6C). Mutations in the ligand binding domain of *ESR1* (1.1%) were
178 extremely rare³ (Supplementary Figure 6A). To uncover novel hotspots in these data, both Chi-
179 squared and Fisher's exact tests were performed using mutation frequencies from previous
180 sequencing studies as the expected values (see Methods for definition of multi-study MAF file)
181 (Supplementary Table 3). The most notable novel finding was in *CBFB* (**Figure 1B**). At least 6
182 different genomic alterations were observed in 15 patients (Supplementary Data 3) that affected
183 the donor splice site of exon 2. Manual review of this splice site identified at least two additional
184 patients with evidence for mutations at this location. The predicted effect of these mutations is
185 skipping of exon 2 or alternate donor site usage, each likely resulting in loss-of-function of the
186 *CBFB* protein. Additional splice site mutations were observed at the exon 2, exon 4 and exon 5
187 acceptor sites of *CBFB*. ErbB2 expressed the anticipated profile of activating mutations from
188 earlier publications⁸ with 22/1259 (1.7%) samples harboring known activating mutations and
189 another 6 variants of unknown significance in the kinase domain or at the S310 residue (**Figure**
190 **8C**).

191

192 Somatic mutation association with PAM50-based intrinsic subtype

193

194 The PAM50 intrinsic subtype calls were obtained from previously published analyses to
195 compare their mutational profiles between UBC-TAM and the MA12 studies. In both studies
196 about half the patients had luminal A tumor. However, the MA12 cohort had a higher proportion
197 of non-luminal subtypes, with 19.8% HER2-E and 6.6% basal and fewer luminal B tumors
198 (25.1% versus 42.4%) (**Figure 2A-B**). Age density plots by subtype serve to emphasize the
199 large difference in the median age between the two sample cohorts (43 versus 65), and also the
200 influence of age with respect to the intrinsic subtype incidence. Namely, in the younger MA12
201 cohort, there is a younger peak incidence with basal-like breast cancer than Luminal A disease
202 (**Figure 2D**). In contrast in the older UBC-TAM cohort, an influence of age on intrinsic subtype
203 was not observed (**Figure 2C**). Relationships between intrinsic subtype and mutation patterns
204 were also explored, classifying mutation positive status as "non-silent", "missense",

205 nonsense/frame-shift (FS/NS) or FS/NS+splice site (Supplementary Data 5). The FDR
206 corrected p-value (q-value) took into account that 83 genes were examined. However, this level
207 of false discovery detection could be viewed as overly conservative in an exploratory analysis
208 and any gene mutation with q-value association of <0.2 was therefore considered reportable ⁹-
209 ¹¹. For MA12, non-silent TP53 mutation was highly subtype-associated because of the very
210 high incidence in non-luminal versus luminal subtypes. PIK3CA and MAP3K1 mutations were
211 associated with Luminal A disease in both cohorts (Supplementary Figure 7A). Finally, there
212 was a strong association between Luminal B status and non-silent (Supplementary Figure 7B)
213 as well as FS/NS mutations in GATA3 (Supplementary Data 5, q value = 0.006). GATA3
214 mutations were present in 28-30% of Luminal B cases and less so in luminal A cases (5%).
215 Considering q values of <0.2 the associations between FS/NS and non-silent mutations in ATM
216 and Luminal B tumors in MA12 (8-13%) suggests that ATM loss is also a possible luminal B
217 driver (Supplementary Figure 7B), at least in younger women (MA12). Relationships between
218 age and mutation incidence were therefore also explored (Supplementary Figure 7C), with the
219 finding that both ATM mutation and GATA3 mutations were associated with an earlier age of
220 onset within the luminal B category (**Figure 2E and 2F**). Finally, NF1 mutations were
221 associated with the HER2-enriched subtype in the UBC-Tam series, explaining the association
222 with poor outcomes (Supplementary Figure 7B).
223

224 Survival analysis according to somatic mutation.
225

226 For the UBC-TAM Series (**Figure 3A**), univariate analysis of favorable prognostic associations
227 for breast cancer specific survival (BCSS) were detected for non-silent mutations in *MAP3K1*,
228 *ERBB3*, *XBP1* and *PIK3CA* (**Figure 3B**, Supplementary Data 6). Adverse prognostic effects
229 were observed for non-silent mutations in *DDR1* and *TP53*, as well as for frame-shift and
230 nonsense (FS/NS) mutations in *NF1*. An analysis for recurrence free survival (RFS) produced
231 similar results, except for *ARID1B*, which was marginally associated with more favorable
232 outcome. A multivariate Cox model was applied to put each gene in the context of clinical
233 parameters (grade, tumor size and node status). These analyses indicated that the prognostic
234 effects of non-silent *DDR1*, *PIK3CA*, *GATA3* FS/NS, *TP53* and *MAP3K1* mutations were
235 independent of grade and pathological stage (**Figure 3C**). Multiple correction testing, yielded
236 *DDR1* as the only gene that remained significant with a q-value of 0.0003. (Supplementary
237 Data 5). For the MA12 clinical trial cohort (**Figure 4A**) we focused on overall survival
238 associations as this was the primary endpoint of the study and the most robust endpoint. A
239 number of rarely mutated genes were associated with poor outcome in univariate analysis as
240 displayed in **Figure 4B**. Multiple testing corrections indicated none of these findings could be
241 considered significant ⁹⁻¹¹. However, in multivariate analysis, based on the uncorrected p value,
242 the prognostic effects of mutations in *ErbB2*, *ErbB4*, *LTK* FS/NS, *MAP3K4*, *PIK3R1*, *RB1*, *RELN*
243 and *TGFB2* were independent of pathological stage and grade (**Figure 4B**).
244

245 Verification of Prognostic effects of Mutations in METABRIC data.
246

247 While few genes were significant in univariate analysis after multiple testing correction, they
248 provide valuable hypotheses for further testing and validation. We therefore sought additional
249 data in the public domain to further assess the uncorrected p value-based findings in our data
250 set. The METABRIC consortium have reported somatic mutations in cBioPortal ¹² with co-
251 reported detailed hormone receptor status, age at diagnosis (median age=64 years for ER+
252 patients), mean follow up of >8 years and disease-specific outcome ^{13, 14}. This data set provided
253 the opportunity to conduct a validation exercise for overlapping genes in the two data sets. For
254 the UBC-TAM series (**Figure 3**), 9 genes with a univariate p value of <0.05 were brought
255 forward for validation (**Figure 5**). Of the 6 overlapping genes also examined in METABRIC,

256 consistent prognostic effects independent of clinical variables were observed for non-silent
257 mutations in three genes, *MAP3K1* (favorable), *TP53* (unfavorable) and *NF1* FS/NS mutations
258 (unfavorable). For the MA12 series (**Figure 4**), 5 shared genes were identified with univariate p
259 values of <0.05 , yet only *PIK3R1* mutations (non-silent or FS/NS) showed consistent adverse
260 prognostic effects (**Figure 6**). The Kaplan Meier survival plots for the consistent adverse
261 prognostic effects of *NF1* FS/NS and non-silent *PIK3R1* mutations are illustrated in **Figure 7A-D**.
262

263
264 Prognostic interactions between *PIK3CA* and *MAP3K1*.
265

266 Since *PIK3CA* and *MAP3K1* mutations co-associate, the combined effect of non-silent
267 mutations in these genes was examined. Patients with tumors exhibiting both genes mutated
268 have a more favorable clinical course than either singly mutant cases or cases without either
269 gene mutated. While the prognostic effects were strongest in the UBC-TAM series, this result
270 was also reproduced in the METABRIC data (**Figure 7E-F**).
271

272 Mutation Analyses for Uncommon Targetable Kinases.
273

274 Of the 83 genes analyzed, at least 8 are directly targetable with small molecules or antibodies
275 that are either FDA approved or in late-stage development (**Figure 8**). Pre-existing data on
276 these mutations is summarized (Supplementary Data 7). *PIK3CA* is not further discussed here,
277 since the mutation spectrum is well-described and large therapeutic studies are already
278 underway. A total of 23 patients with breast cancer with ErbB2 activating mutations were
279 identified. An examination of their locations revealed that ErbB2 mutations were, as expected,
280 clustered in 2 major domains, with 2 of 23 having extracellular domain mutations at residue 310
281 and 21 of 23 having kinase domain mutations between residues 755-842^{8, 15}. To further
282 investigate the preliminary finding of an adverse prognostic effect for ErbB2 mutation in the
283 MA12 series, an examination of the METABRIC data indicated that known activating mutations
284 in ErbB2 were associated with a near significant adverse effect (HR=1.71, P=0.075)
285 (Supplementary Figure 8). For ERBB3, 2 known-activating mutations were identified (V104L
286 and E928A)¹⁶. The DDR1 kinase domain mutation, R776W, is possibly homologous to EGFR
287 hot spot mutation L858R, but the remaining DDR1 variants are of unknown significance. For the
288 mutations in JAK1, 3 of 12 are loss of function mutations (frame shift or non-sense) and the
289 S816* mutation has been reported in a lung adenocarcinoma sequencing data set¹⁷. The loss
290 of function mutations in JAK1 have been shown to associate with immune therapy resistance^{18,}
291¹⁹. A few mutations identified in ERBB4, MET, and PDGFRA have been previously reported but
292 those reported here have not been functionally tested.
293
294

295 Discussion

296
297 The landscape of recurrently mutated genes in ER+ breast cancer observed in this study is
298 consistent with reports where matched germline samples were available, indicating that our
299 variant filters were effective for somatic mutation detection in a research setting. Overall,
300 mutation rates were higher in our cohort (e.g., for *PIK3CA*, *MLL3*, *MAP3K1*) than the TCGA
301 cohort, but were also lower for a few specific genes (e.g., *TP53* and *GATA3*). Due to higher
302 sequencing data coverage of recurrently mutated target genes than TCGA and the use of a
303 different hybrid capture reagent, we were likely able to detect mutations that were missed with
304 lower-depth exome or whole genome sequencing data. It is also possible that in some instances
305 we overestimated somatic mutation rates, due to the lack of matched normal samples and
306 imperfections in our germline polymorphism filtering. In particular, a significant number of

307 BRCA1 and BRCA2 mutations are likely *de novo* germline mutations that we would not be able
308 to easily distinguish from somatic mutations. Of the 117 non-silent BRCA1/2 mutations
309 observed (from 110/1128 patients; 7 patients had two hits) 74 were observed at a VAF greater
310 than 40% and 31 were greater 60%. Variants with VAFs this high are less likely to be somatic
311 given the general expectation of impure tumor samples and heterozygous mutations. Indeed,
312 the VAFs for BRCA1/2 non-silent mutations (mean=44.8%) were significantly higher than for
313 other genes (mean=36.4%, p = 6.96e-06). There were 8 known pathogenic (ENIGMA expert
314 reviewed) mutations according to a search of the BRCA Exchange database
315 (<http://brcaexchange.org>, Nov 12, 2017) and another 37 likely pathogenic (FS/NS) mutations. Of
316 the remaining, 4 were known benign according to expert review (ENIGMA), and 8 benign, 15
317 likely benign and 45 variants of unknown significance according to all public sources.
318

319 The discovery of a novel recurrent *CBFB* (core binding factor subunit beta) splice site mutation
320 in this cohort illustrates a limitation of exome capture reagents. The affected bases in exon 2 of
321 *CBFB* display reduced sequence coverage, possibly due to high GC content, in the breast
322 TCGA exome dataset (Supplementary Figures 9-10). This site was mutated in at least 1.5% of
323 ER+ breast cancers sequenced, bringing the overall rate of *CBFB* mutations to nearly 6%,
324 which should drive further investigation of this gene in ER+ breast cancer pathogenesis. *CBFB*
325 functions as a subunit in a heterodimeric core binding transcription factor that interacts with
326 *RUNX1*²⁰. Consistent with this model, *CBFB* mutants were mutually exclusive from *RUNX1*
327 mutants in this cohort with only a single sample harboring non-silent mutations in both *CBFB*
328 and *RUNX1*.
329

330 The UBC-TAM and MA12 studies revealed different lists of potentially prognostic mutations.
331 Prognostic effects are likely to be strongly affected by the use of systemic therapy as well as by
332 patient age at diagnosis. The UBC-TAM series is the simplest study to interpret from a drug
333 resistance perspective since the only systemic therapy was tamoxifen. Thus, the consistent
334 adverse effect of NF1 FS/NS mutation on prognosis is intriguing as this result is consistent with
335 results from an *in vitro* screen for tamoxifen resistance²¹. Understanding why only FS/NS
336 mutations predict poor outcome, rather than missense or other non-silent mutations, will require
337 further investigation. In contrast, PIK3R1 mutation emerged as a consistent poor prognosis
338 mutation from the MA12 analysis, with validation in METABRIC. The proposed favorable
339 prognostic effects of PIK3CA mutation were observed in the UBC-TAM series, but were not
340 found to be independent of stage and grade, and PTEN mutations were neutral.
341

342 According to our validation results, NF1, PIK3R1, MAP3K1, PIK3CA and TP53 are likely to be
343 prognostic drivers. In postmenopausal women treated with adjuvant endocrine therapy, DDR1,
344 PRKDC and XBP1 should be further studied and of these DDR1 is the strongest candidate
345 because it was significant despite strict false discovery correction. DDR1 is a collagen-binding
346 receptor expressed in epithelial cells that stabilizes E-cadherin-mediated intracellular
347 adhesion²². DDR1 mutations also occur in endometrial cancer²³, acute leukemia²⁴ and lung
348 cancer²⁵. Loss of DDR1 (DDR1-null mice) produces hyper-proliferation and abnormal branching
349 of mammary ducts, suggesting DDR1 is a breast tumor suppressor²⁶. The relationship between
350 truncating mutations in NF1 and poor outcome is consistent with an siRNA screen for genes
351 whose loss generates tamoxifen resistance²¹. Mutations in PRKDC will potentially produce a
352 defective ATM response/low ATM levels²⁷ which is interesting in the context of the finding
353 herein that ATM mutations are a potential luminal B driver gene. The significance of a defective
354 ATM pathway as a cause of endocrine resistance is highlighted by the recent finding that
355 dysregulation of the MutL complex (MLH1, PMS1 and PMS2) causes failure of ATM/CHK2-
356 based negative regulation of CDK4/6²⁸. Prognostic candidate mutations revealed by the MA12
357 analysis were different from the UBC TAM series, likely reflecting the different patient profiles

358 and adjuvant treatments illustrated in **Figure 2**. The prognostic effects of mutations ERBB2,
359 ERBB4, JAK1, LTK, MAP3K4, MET, PDGFRA, RB1, RELN, TGFB2, all await further study with
360 even larger sample sizes.

361
362 In conclusion, we have successfully utilized clinically well-annotated, uniformly treated patient
363 samples using DNA from archival material greater than 20 years old that lacks a matched
364 normal to explore the prognostic effects encoded by the mutational landscape of ER+ breast
365 cancer. We were able to confirm our prospective hypothesis that MAP3K1 is associated with
366 indolent disease and TP53 with adverse outcomes. We also associated NF1 FS/NS mutations
367 with strong adverse effects on prognosis. Similarly, PIK3R1 mutations were associated with an
368 adverse prognosis in contrast to PIK3CA mutation. This suggests somatic mutations in these
369 two physically interacting gene products are not biologically equivalent with respect to PI3
370 kinase pathway activation and resistance effects. The possibility that the long tail of low
371 frequency mutation events in luminal type breast cancer may harbor multiple molecular
372 explanations for poor outcomes is an important finding that should spur collaborative efforts to
373 thoroughly screen thousands of properly annotated cases. Only after these iterative efforts of
374 proposing and confirming candidates will a clinically useful and comprehensive somatic
375 mutation-based classification of ER+ breast cancer emerge. In the meantime, functional studies
376 should be pursued to understand the biological effects of somatic mutations, prioritizing these
377 studies according to whether the mutations are driving an adverse prognostic effect.

378
379 **Methods**
380

381 For the UBC-TAM series, an institutional review board approved study was based on formalin-
382 fixed paraffin embedded (FFPE) primary tumor blocks from 947 female patients diagnosed with
383 estrogen receptor positive invasive breast cancer in the province of British Columbia in Canada
384 between 1986 and 1992^{6, 29-31}. The sample flow and analysis are provided in a REMARK
385 summary (**Figure 3A**). DNA was isolated from tumor-rich regions using the Qiagen blood and
386 tissue kit, which yielded sufficient DNA in 645 samples, of which 625 met all study criteria and
387 had sufficient sequence coverage. Similarly, approved studies provided 194 and 454 HR+
388 patient samples for the POLAR and MA12 (**Figure 4A**) cohorts. A total of 175 POLAR and 459
389 (328 HR+) MA12 samples yielded sufficient DNA and had sufficient sequence coverage for
390 analysis. Detailed descriptions of the patient data sets are provided in Supplementary Table 3.
391 A meta-analysis of six existing published large-scale breast cancer sequencing studies^{1-3, 5, 32, 33}
392 was performed to identify genes with recurrent coding region somatic mutations in breast cancer
393 (Supplementary Data 1). Additional drug targets³⁴ and genes with relevance to breast cancer
394 from targeted sequencing³⁵, copy-number studies¹³ or knowledge relating to somatic or germline
395 mutations (e.g., *BRCA1*, *BRCA2*, *ERBB2*, *ESR1* and *PRLR*) were also included. This resulted in
396 a final list of 83 breast-cancer-related genes (Supplementary Table 1). These genes were
397 targeted comprehensively with 3,029 complementary probes for hybridization-based enrichment
398 (Supplementary Data 8). Sequencing libraries were constructed, hybridized with capture probes,
399 multiplexed and run on a single flow cell with up to 96 samples per pool per lane yielding
400 approximately 375 Mb of DNA sequence per sample from an Illumina HiSeq paired end 2 X
401 100bp (TAM) or 2 X 125bp (POLAR, MA12) sequencing run following manufacturer's protocols.

402
403 Variant calling was performed with the Genome Modeling System as previously described³⁶.
404 Specifically, sequence data were aligned to reference sequence build GRCh37 using BWA³⁷
405 and de-duplicated with Picard. SNVs and indels were detected using the union of samtools³⁸
406 and VarScan2⁵ and annotated using Ensembl version 70. Variants were restricted to the coding
407 regions of targeted genes and filtered for false positives and germline polymorphisms against a
408 database of nearly 70,000 unmatched normals from the ExAC consortium, 1000 Genomes³⁹,

409 NHLBI exomes⁴⁰ and TCGA data sets^{3, 41}. A binomial probability model was then applied to the
410 variants using VAF and total coverage to determine a log-likelihood ratio of being a somatic
411 variant as previously described⁴² (See Supplementary Methods). After filtering, all remaining
412 variants were manually reviewed. To ensure that variants of known clinical relevance were not
413 missed by automated variant calling approaches, a knowledge-based variant calling strategy
414 was performed focused on the mutations in the Database of Curated Mutations⁴³.
415

416 Patient groups were defined by mutation status or truncating mutation status for each gene.
417 Fisher's exact and Chi-squared tests were used for hotspot analysis, mutual exclusivity or co-
418 occurrence, and other categorical clinical statistics (e.g., mutation status vs. intrinsic subtype) as
419 appropriate. Univariate Kaplan-Meier and Cox survival analyses were performed for breast-
420 cancer-specific survival (BCSS), relapse free survival (RFS), or overall survival (OS) with non-
421 silent or truncating mutation status as a factor. Significant survival differences between the
422 groups were determined by log rank (Mantel-Cox) test. The Benjamini-Hochberg method was
423 performed for multiple testing corrections to report the false discovery rate adjusted p-value (q-
424 value). A multivariate Cox proportional hazard model was fitted to BCSS and RFS separately on
425 gene mutation status, node status, grade and tumor size and adjusted hazard ratios were
426 calculated with Wald test p-values. All statistical analyses were performed in the R statistical
427 programming language with core, 'survival' and 'multtest' libraries. Genomic visualizations were
428 created with ProteinPaint⁴⁴ and GenVisR⁴⁵.
429
430
431
432
433

434

435

References

- 436 1. Banerji, S. et al. Sequence analysis of mutations and translocations across breast
437 cancer subtypes. *Nature* **486**, 405-409 (2012).
- 438 2. Stephens, P.J. et al. The landscape of cancer genes and mutational processes in breast
439 cancer. *Nature* **486**, 400-404 (2012).
- 440 3. Cancer Genome Atlas, N. Comprehensive molecular portraits of human breast tumours.
441 *Nature* **490**, 61-70 (2012).
- 442 4. Kennecke, H.F. et al. Late risk of relapse and mortality among postmenopausal women
443 with estrogen responsive early breast cancer after 5 years of tamoxifen. *Ann Oncol* **18**,
444 45-51 (2007).
- 445 5. Ellis, M.J. et al. Whole-genome analysis informs breast cancer response to aromatase
446 inhibition. *Nature* **486**, 353-360 (2012).
- 447 6. Nielsen, T.O. et al. A comparison of PAM50 intrinsic subtyping with
448 immunohistochemistry and clinical prognostic factors in tamoxifen-treated estrogen
449 receptor-positive breast cancer. *Clin Cancer Res* **16**, 5222-5232 (2010).
- 450 7. Samuels, Y. et al. High frequency of mutations of the PIK3CA gene in human cancers.
451 *Science* **304**, 554 (2004).
- 452 8. Bose, R. et al. Activating HER2 mutations in HER2 gene amplification negative breast
453 cancer. *Cancer Discov* **3**, 224-237 (2013).
- 454 9. Amar, D., Shamir, R. & Yekutieli, D. Extracting replicable associations across multiple
455 studies: Empirical Bayes algorithms for controlling the false discovery rate. *PLoS
456 Computational Biology* **13**, e1005700 (2017).
- 457 10. Capanu, M. & Seshan, V.E. False discovery rates for rare variants from sequenced data.
458 *Genetic epidemiology* **39**, 65-76 (2015).
- 459 11. Efron, B. Size, Power and False Discovery Rates. *The Annals of Statistics* **35**, 1351-
460 1377 (2007).
- 461 12. Gao, J. et al. Integrative analysis of complex cancer genomics and clinical profiles using
462 the cBioPortal. *Sci Signal* **6**, pl1 (2013).
- 463 13. Curtis, C. et al. The genomic and transcriptomic architecture of 2,000 breast tumours
464 reveals novel subgroups. *Nature* **486**, 346-352 (2012).
- 465 14. Pereira, B. et al. The somatic mutation profiles of 2,433 breast cancers refines their
466 genomic and transcriptomic landscapes. *Nat Commun* **7**, 11479 (2016).
- 467 15. Ma, C.X. et al. Neratinib Efficacy and Circulating Tumor DNA Detection of HER2
468 Mutations in HER2 Nonamplified Metastatic Breast Cancer. *Clin Cancer Res* **23**, 5687-
469 5695 (2017).
- 470 16. Jaiswal, B.S. et al. Oncogenic ERBB3 mutations in human cancers. *Cancer Cell* **23**,
471 603-617 (2013).
- 472 17. Iminielski, M. et al. Mapping the hallmarks of lung adenocarcinoma with massively
473 parallel sequencing. *Cell* **150**, 1107-1120 (2012).
- 474 18. Shin, D.S. et al. Primary Resistance to PD-1 Blockade Mediated by JAK1/2 Mutations.
475 *Cancer Discov* **7**, 188-201 (2017).
- 476 19. Zaretsky, J.M. et al. Mutations Associated with Acquired Resistance to PD-1 Blockade in
477 Melanoma. *N Engl J Med* **375**, 819-829 (2016).
- 478 20. Lukasik, S.M. et al. Altered affinity of CBF beta-SMMHC for Runx1 explains its role in
479 leukemogenesis. *Nat Struct Biol* **9**, 674-679 (2002).
- 480 21. Mendes-Pereira, A.M. et al. Genome-wide functional screen identifies a compendium of
481 genes affecting sensitivity to tamoxifen. *Proc Natl Acad Sci U S A* **109**, 2730-2735
482 (2012).

483 22. Yeh, Y.C., Wu, C.C., Wang, Y.K. & Tang, M.J. DDR1 triggers epithelial cell
484 differentiation by promoting cell adhesion through stabilization of E-cadherin. *Molecular*
485 *biology of the cell* **22**, 940-953 (2011).

486 23. Rudd, M.L. et al. Mutational analysis of the tyrosine kinase in serous and clear cell
487 endometrial cancer uncovers rare somatic mutations in TNK2 and DDR1. *BMC Cancer*
488 **14**, 884 (2014).

489 24. Loriaux, M.M. et al. High-throughput sequence analysis of the tyrosine kinase in acute
490 myeloid leukemia. *Blood* **111**, 4788-4796 (2008).

491 25. Ding, L. et al. Somatic mutations affect key pathways in lung adenocarcinoma. *Nature*
492 **455**, 1069-1075 (2008).

493 26. Vogel, W.F., Aszodi, A., Alves, F. & Pawson, T. Discoidin domain receptor 1 tyrosine
494 kinase has an essential role in mammary gland development. *Molecular and cellular*
495 *biology* **21**, 2906-2917 (2001).

496 27. Peng, Y. et al. Deficiency in the catalytic subunit of DNA-dependent protein kinase
497 causes down-regulation of ATM. *Cancer Res* **65**, 1670-1677 (2005).

498 28. Haricharan, S. et al. Loss of MutL Disrupts CHK2-Dependent Cell-Cycle Control through
499 CDK4/6 to Promote Intrinsic Endocrine Therapy Resistance in Primary Breast Cancer.
500 *Cancer Discov* **7**, 1168-1183 (2017).

501 29. Cheang, M.C. et al. Ki67 index, HER2 status, and prognosis of patients with luminal B
502 breast cancer. *J Natl Cancer Inst* **101**, 736-750 (2009).

503 30. Liu, S. et al. Prognostic significance of FOXP3+ tumor-infiltrating lymphocytes in breast
504 cancer depends on estrogen receptor and human epidermal growth factor receptor-2
505 expression status and concurrent cytotoxic T-cell infiltration. *Breast Cancer Res* **16**, 432
506 (2014).

507 31. Parker, J.S. et al. Supervised risk predictor of breast cancer based on intrinsic subtypes.
508 *J Clin Oncol* **27**, 1160-1167 (2009).

509 32. Kan, Z. et al. Diverse somatic mutation patterns and pathway alterations in human
510 cancers. *Nature* **466**, 869-873 (2010).

511 33. Shah, S.P. et al. The clonal and mutational evolution spectrum of primary triple-negative
512 breast cancers. *Nature* **486**, 395-399 (2012).

513 34. Griffith, M. et al. DGIdb: mining the druggable genome. *Nat Methods* **10**, 1209-1210
514 (2013).

515 35. Chanock, S.J. et al. Somatic sequence alterations in twenty-one genes selected by
516 expression profile analysis of breast carcinomas. *Breast Cancer Res* **9**, R5 (2007).

517 36. Griffith, M. et al. Genome Modeling System: A Knowledge Management Platform for
518 Genomics. *PLoS Comput Biol* **11**, e1004274 (2015).

519 37. Li, H. & Durbin, R. Fast and accurate short read alignment with Burrows-Wheeler
520 transform. *Bioinformatics* **25**, 1754-1760 (2009).

521 38. Li, H. et al. The Sequence Alignment/Map format and SAMtools. *Bioinformatics* **25**,
522 2078-2079 (2009).

523 39. Genomes Project, C. et al. A map of human genome variation from population-scale
524 sequencing. *Nature* **467**, 1061-1073 (2010).

525 40. Fu, W. et al. Analysis of 6,515 exomes reveals the recent origin of most human protein-
526 coding variants. *Nature* **493**, 216-220 (2013).

527 41. Cancer Genome Atlas Research, N. Genomic and epigenomic landscapes of adult de
528 novo acute myeloid leukemia. *N Engl J Med* **368**, 2059-2074 (2013).

529 42. Krysiak, K. et al. A genomic analysis of Philadelphia chromosome-negative AML arising
530 in patients with CML. *Blood Cancer J* **6**, e413 (2016).

531 43. Ainscough, B.J. et al. DoCM: a database of curated mutations in cancer. *Nat Methods*
532 **13**, 806-807 (2016).

533 44. Zhou, X. et al. Exploring genomic alteration in pediatric cancer using ProteinPaint. *Nat Genet* **48**, 4-6 (2016).
534 45. Skidmore, Z.L. et al. GenVisR: Genomic Visualizations in R. *Bioinformatics* **32**, 3012-3014 (2016).

537
538
539
540
541

542 Acknowledgements:

543

544 Research reported in this publication was primarily supported by Susan G. Komen Promise
545 grant (PG12220321 to MJE), a Cancer Prevention and Research Institute of Texas (CPRIT)
546 Recruitment of Established Investigators award (RR140033 to MJE). Dr. Ellis is a McNair
547 Medical Institute Investigator and a Susan G. Komen Scholar. SMK was supported by a Komen
548 CCR award (CCR16380599). The MA12 analysis was supported by research grants from
549 Canadian Cancer Society Research Institute to the NCIC Clinical Trials Group (021039 and
550 015469). OLG was supported by the National Cancer Institute (NIH NCI K22CA188163 and
551 NIH NCI U01CA209936).

552

553

554 Contributions:

555

556 O.L.G., N.C.S., T.O.N., M.J.E., E.R.M. designed the experiments; M.G., J. K., C.A.M., K.K.,
557 J.H., B.J.A., Z.L.S., K.C. R.K. C.F., L.C., J.E.S., S.D., V.M., D.E.L., R.S.F., S.L., R.K.W.
558 generated the sequencing data, T.O.N., B.Y., M.D. S.L., and D.V. orchestrated the sample
559 pipeline., M.A., O.L.G. and N.C.S., prepared the figures and tables. M.A., J.L., and D.T.
560 provided statistical analysis. S.M.K., R.B., and E.C.C. provided functional annotations., T.O.N
561 provided pathology analysis. M.J.E., N.C.S., M.A., and O.L.G. wrote the manuscript. E.R.M.,
562 T.O.N., M.D., critically read and commented on the manuscript.

563

564 Conflict of Interest:

565

566 Dr. Ellis and Dr. Mardis report income on patents on the PAM50 intrinsic subtype algorithm. Dr.
567 Ellis reports ownership in Bioclassifier LLC that licenses PAM50 patents to Nanostring for the
568 Prosigna breast cancer prognostic test. Commercial platforms and algorithms were not used in
569 the analyses reported in this paper.

570

571 Figure Legends

572

573 **Figure 1. Mutation recurrence and novel splice site mutation**

574 A) The overall mutation recurrence rate ranged from 41.1% of samples for *PIK3CA* to 0.0% for
575 *PIN1*. The figure depicts non-silent mutations for all 1128 patients for the top 16 most
576 recurrently mutated genes (>5% recurrence). If a patient had multiple mutations it is colored
577 according to the “most damaging” mutation following the order presented in the Mutation Type
578 legend (vertical color bar). Mutations per MB were calculated using the total number of
579 mutations observed over the total exome space corresponding to the tiled space from “SeqCap
580 EZ Human Exome Library v2.0”. A correction factor was applied for genes not assayed using
581 the expected number of additional mutations based on TCGA data. B) Mutation recurrence
582 rates (amino acid level) in this study were compared to previously reported mutation rates from
583 a multi-study MAF file of six reported breast cancer sequencing studies (Supplementary Data
584 1). An entirely novel mutation “hot spot” was discovered affecting the exon 2 splice (donor) site
585 of *CBFB* in at least 15 patients. Six different single nucleotide substitutions, insertions and
586 deletions were observed, all affecting either the first or second base of the donor splice site.
587 These mutations were most likely missed in previous studies because of a lack of sequencing
588 coverage due to the GC-rich nature of exons 1 and 2 of *CBFB* (Supplementary Figures 9-10).
589 Such mutations are predicted to significantly alter the canonical donor site and result in either
590 alternate donor usage or skipping of one or more exons of *CBFB*.

591

592 **Figure 2. Cross-cohort age and subtype analysis**

593 A-B) Percentage composition of samples by intrinsic subtype of the tumor in the two discovery
594 cohorts for UBC-TAM (A) and MA12 (B) cohorts. C-D) Age-density plots for patients categorized
595 by intrinsic subtype in UBC-TAM (C) and MA12 (D) cohorts. The overall median age shows that
596 UBC-TAM is constituted mostly of post-menopausal patients (median age=65), in contrast to
597 MA12, which has younger patients (median age=43). E-F) Younger luminal B subtype patients
598 harbor GATA3 (E) and ATM (F) mutations in the combined set of UBC-TAM and MA12 Luminal
599 B cases (median age=52, p=0.01; median age=58, p=0.03 for GATA3 and ATM respectively).

600

601 **Figure 3. Candidate discovery from UBC-TAM cohort and prognosis evaluation**

602 (A) DNA was extracted from tumor specimens from 947 patients with ER+ breast cancer treated
603 with tamoxifen monotherapy for 5 years. 632 samples with adequate yield were sequenced for
604 83 genes known to be recurrently mutated or breast cancer relevant. A total of 625 samples
605 passed minimum quality checks and were sequenced to an average of 135.8X coverage. A total
606 of ~62 million variants from the reference genome were identified. Extensive filtering and
607 manual review reduced this list to 1,991 putatively somatic variants. Survival analysis was
608 applied to non-silent and truncating gene mutation status versus disease outcome (relapse or
609 breast-cancer-specific death). In addition, mutations were analyzed for novel hotspots, patterns
610 of mutual exclusivity or co-occurrence and association with clinical variables. (B) Forest plot of
611 impact of mutations in candidate genes, identified using UBC-TAM population, on breast-
612 cancer-specific-survival (red) and recurrence-free survival (blue). The variant types are
613 characterized based on non-silent or nonsense/frameshift (FS/NS) mutations. The box size is
614 relative to frequency of mutations listed in the analysis, larger boxes represent high incidence
615 rate mutations. (C) Multivariate forest plot of effect of mutations in UBC-TAM candidate genes
616 on breast cancer specific-survival when assessed together with clinical factors including Tumor
617 Grade, Node positivity and Tumor Size (>5cm).

618

619 **Figure 4. Candidate discovery from MA12 cohort and prognosis evaluation**

620 (A) DNA was extracted from tumor specimens and 470 samples with adequate yield were
621 sequenced for 83 genes known to be recurrently mutated or breast cancer relevant. A total of
622 459 (328 HR+) samples passed minimum quality checks and were sequenced to an average of
623 272.6X coverage. A total of 406 million variants from the reference genome were identified.
624 Extensive filtering and manual review reduced this list to 2104 putatively somatic variants.
625 Survival analysis was applied to non-silent and truncating gene mutation status versus overall
626 survival. (B) Forest plot showing effect of mutation in candidate genes on overall survival
627 (univariate - blue, multivariate - orange), along with the clinical factors used in the multivariate
628 analysis, tumor grade, node positivity and tumor size (>5cm) in black. The box size is relative to
629 frequency of mutations listed in the analysis, larger boxes represents high incidence rate
630 mutations. Note: a few boxes are not shown if their hazard ratio were greater than 4.0.
631

632 **Figure 5. Validation of UBC-TAM candidates in ER+ METABRIC**

633 A) Six out of nine candidate genes from UBC-TAM analysis had mutations reported in
634 METABRIC cohort. 1060 ER+ samples with disease-specific survival information were used to
635 test the effect of mutations in the candidate genes on prognosis. B) Forest plot shows effect of
636 mutated candidate genes on disease-specific survival in METABRIC ER+ cohort with univariate
637 cox proportional-hazard ratio in blue and multivariate in orange. The clinical factors used in the
638 multivariate analysis, namely tumor grade, node positivity and tumor size (>5cm), are shown in
639 black. The box size is relative to frequency of mutations listed in the analysis, larger boxes
640 represent genes with higher incidence rate of mutations.
641

642 **Figure 6. Validation of MA12 candidates in ER+ METABRIC**

643 A) Five out of eleven candidates from MA12 analysis had mutations reported in the METABRIC
644 cohort. 1415 ER+ samples with overall survival information was used to test the effect of
645 mutations in the candidate genes on prognosis. B) Forest plot shows effect of mutated
646 candidate genes, shortlisted based on MA12 mutation analysis, on overall survival in
647 METABRIC ER+ breast cancer patients. Univariate (blue) and multivariate (orange) cox
648 proportional-hazard ratio depict the independent prediction of survival outcomes for the six
649 candidate genes. The box size is relative to frequency of mutations listed in the analysis, larger
650 boxes represent genes with higher incidence rate of mutations.
651

652 **Figure 7. Kaplan-Meier plots**

653 A-B) Kaplan-Meier graph showing the prognostic role of NF1 mutations, separated by variant
654 type – Missense (MUT MS, green), Frameshift/Nonsense (MUT FS/NS, blue) in ER+ breast
655 cancer patients from A) UBC-TAM and B) METABRIC cohort establishing the association
656 between FS/NS mutations in NF1 with poor prognosis. C-D) Kaplan-Meier graph showing the
657 prognostic role of PIK3R1 in C) MA12 and D) METABRIC ER+ breast cancer patients,
658 categorized based on tumors with wildtype (WT, black) or mutated PIK3R1 non-silent mutations
659 (MUT, red). E-F) Kaplan-Meier graph demonstrating co-occurrence of non-silent mutations in
660 MAP3K1 and PIK3CA (red) in E) UBC-TAM and F) METABRIC associates with better survival
661 when compared against tumors with mutations exclusively in MAP3K1 (blue) or PIK3CA (green)
662 or wildtype for both MAP3K1 and PIK3CA (black). p, log rank (Mantel-Cox) test p-value.
663

664 **Figure 8. Mutation profiles for selected genes**

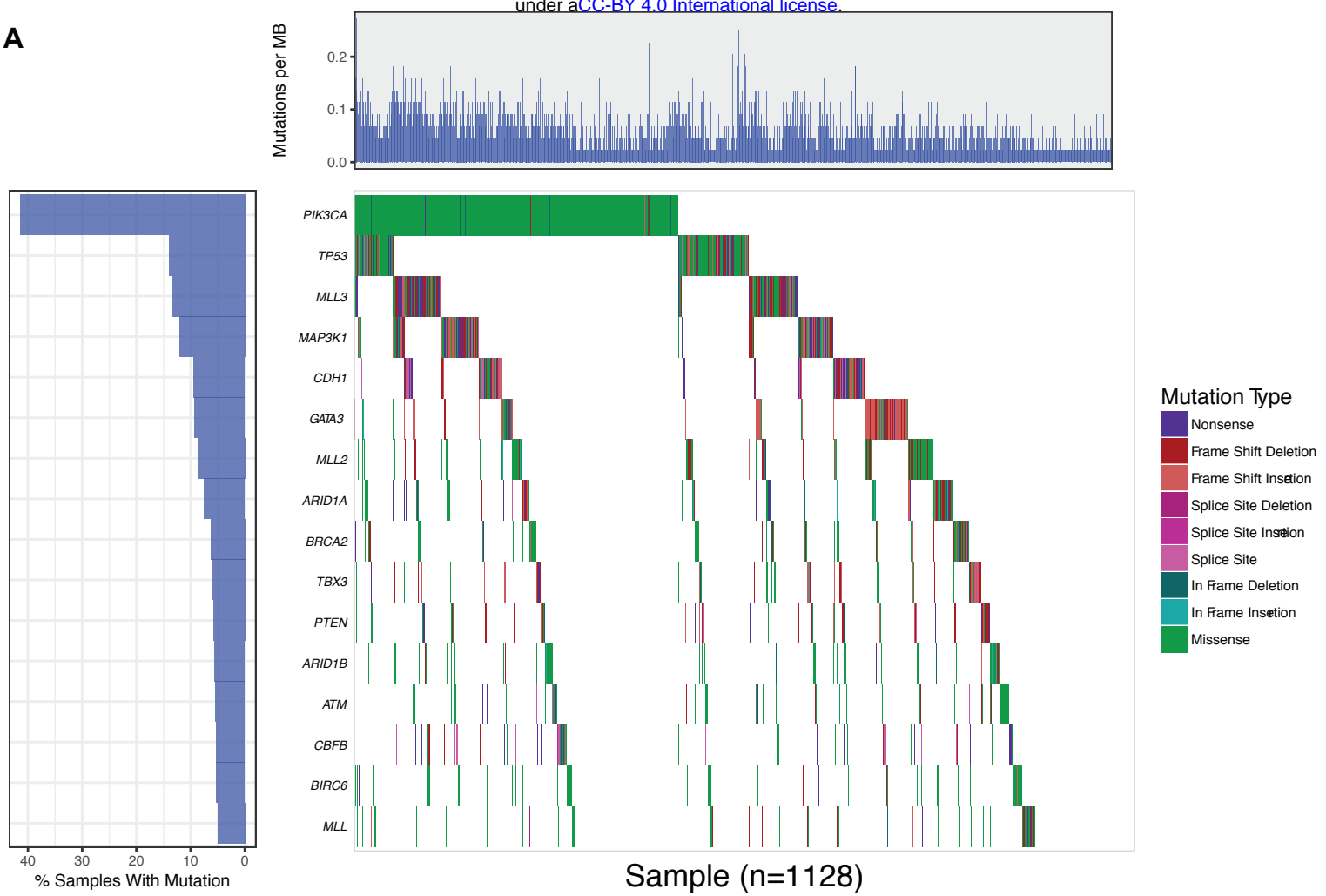
665 Mutation frequency plots illustrate all non-silent mutations (TAM, POLAR, and MA12; n=1259)
666 for representative transcripts for several kinase genes of interest. The domains belonging to A)
667 DDR1 (RefSeq ID: NM_013994) and B) JAK1 (NM_002227) are indicated below the schematic
668 diagram of each gene. The ECD (extracellular domain), TM (transmembrane domain), and
669 kinase domain are depicted as green, red, and orange bars respectively for C) ERBB2
670 (NM_004448), D) ERBB3 (NM_001982), E) ERBB4 (NM_005235), F) MET (NM_000245), and

671 G) PDGFRA (NM_006206). The variant counts across the three datasets for each gene are
672 provided below the gene's name. Note, in the mapping from Ensembl (**Supplementary Data 3**)
673 to RefSeq annotations (required for use of ProteinPaint tool) a small number of variants
674 annotations may have changed or been lost, despite selecting the most similar representative
675 transcript possible.
676

Figure 1.

bioRxiv preprint doi: <https://doi.org/10.1101/235846>; this version posted December 19, 2017. The copyright holder for this preprint (which was not certified by peer review) is the author/funder, who has granted bioRxiv a license to display the preprint in perpetuity. It is made available under aCC-BY 4.0 International license.

A



B

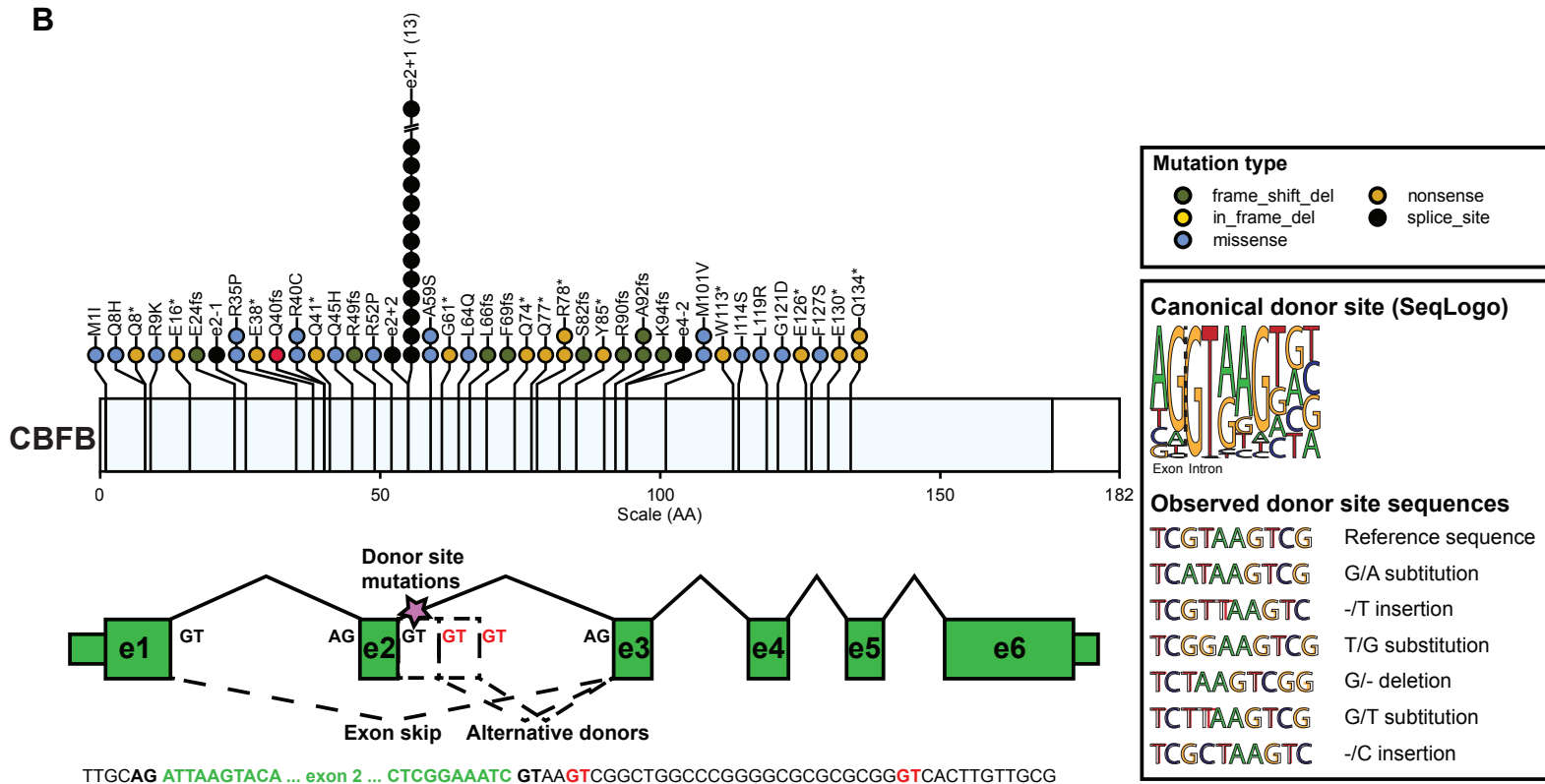


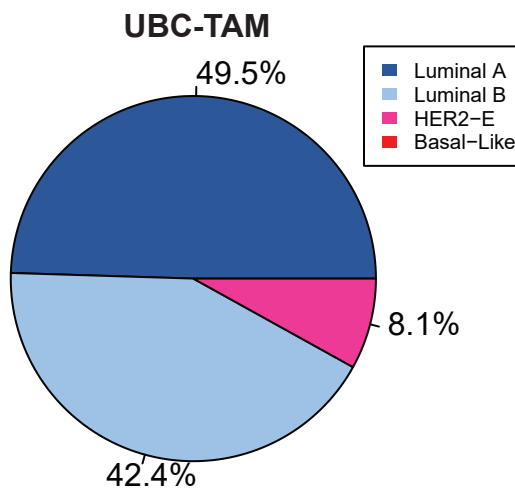
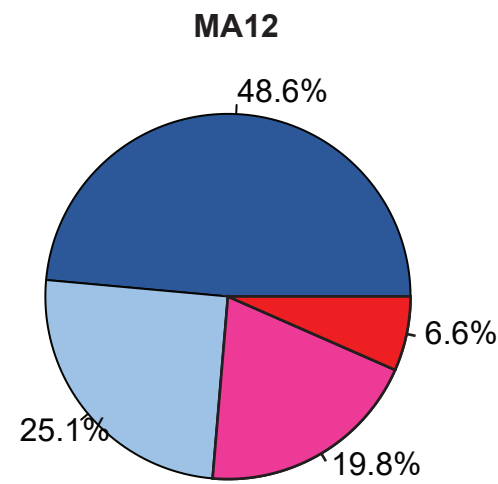
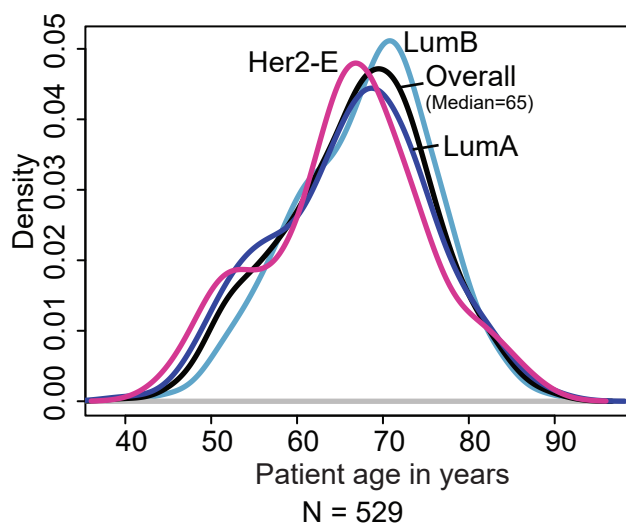
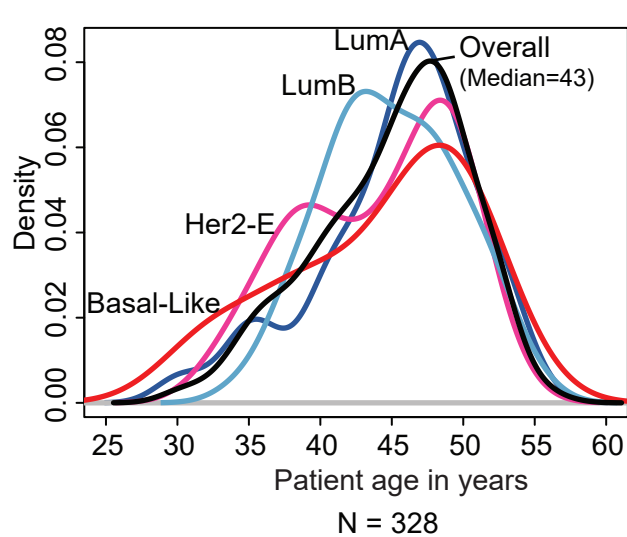
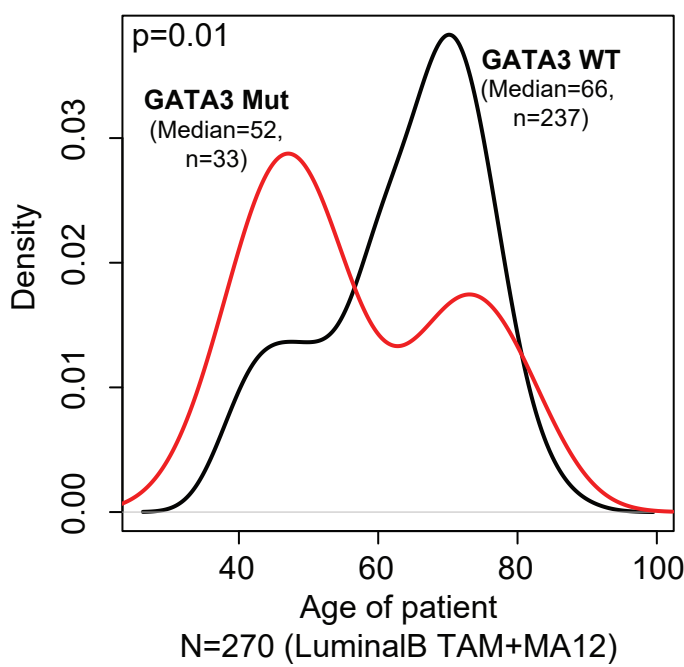
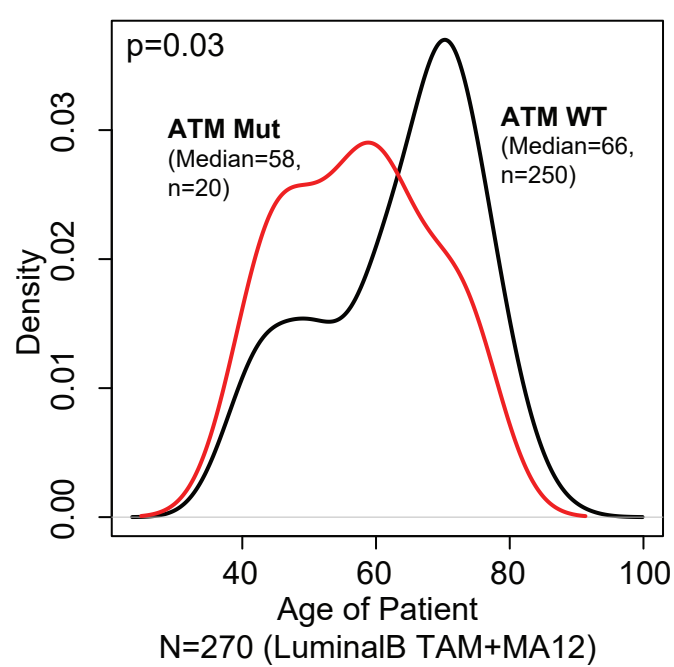
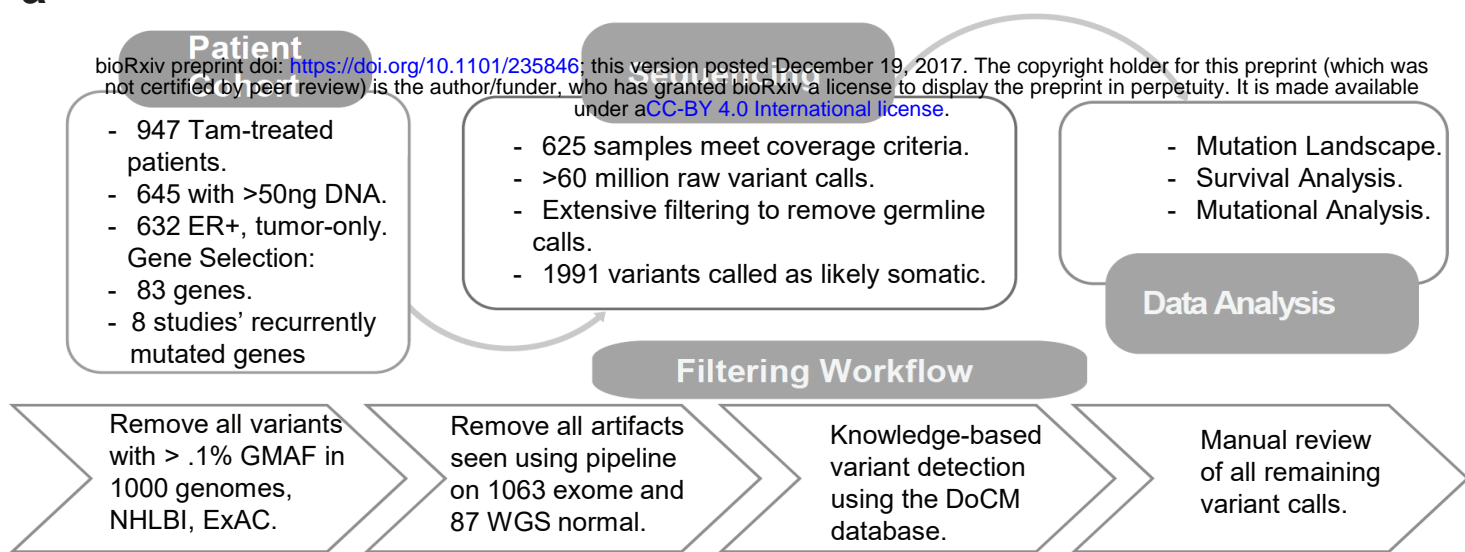
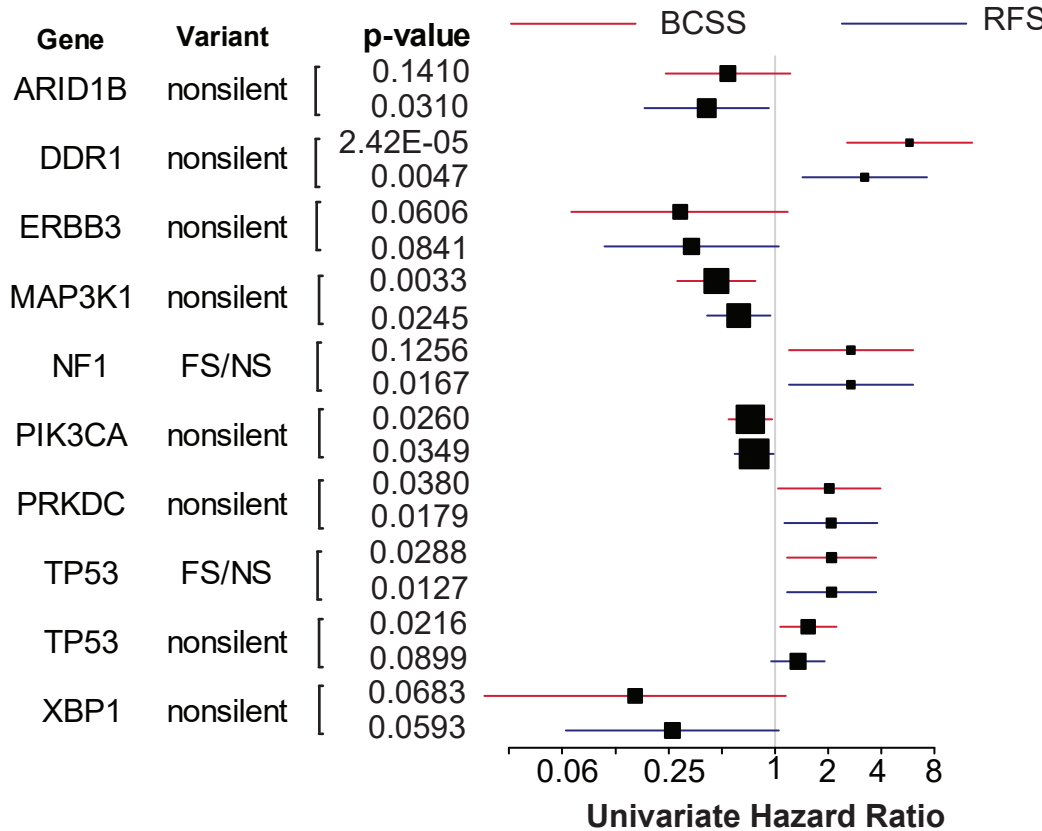
Figure 2.**a****b****c****d****e****f**

Figure 3.

a



b



c

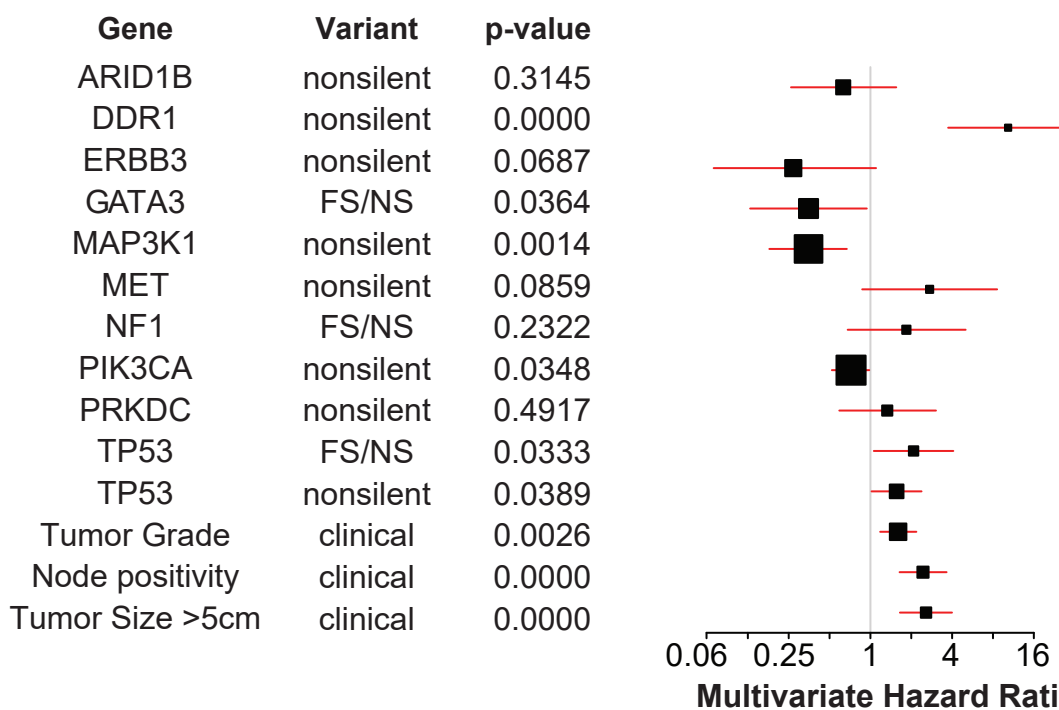


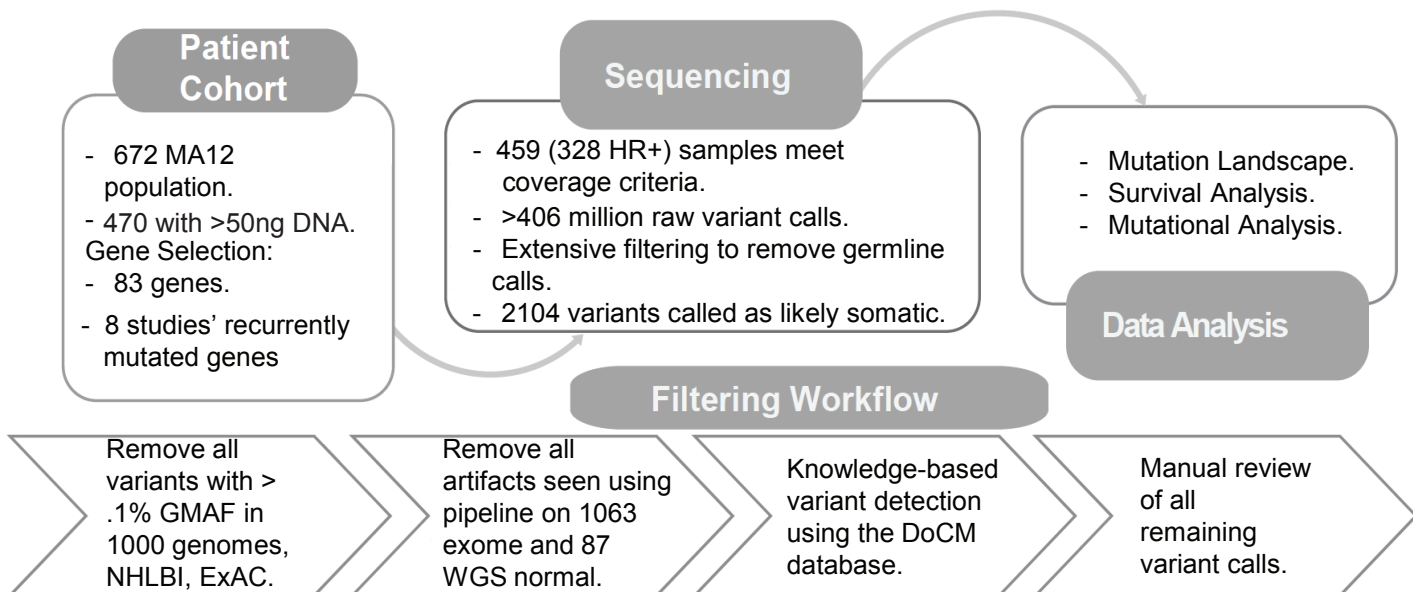
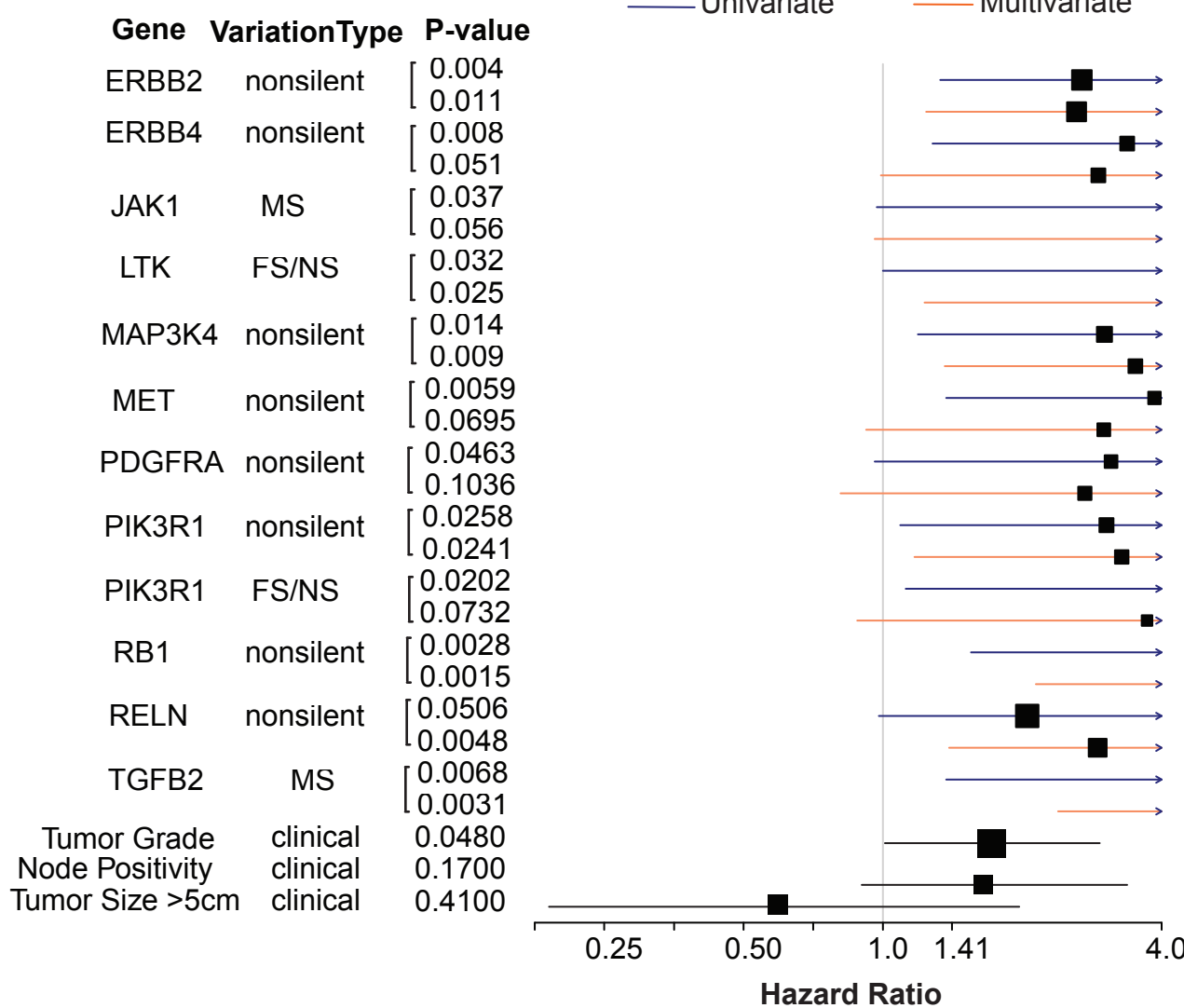
Figure 4.**a****b**

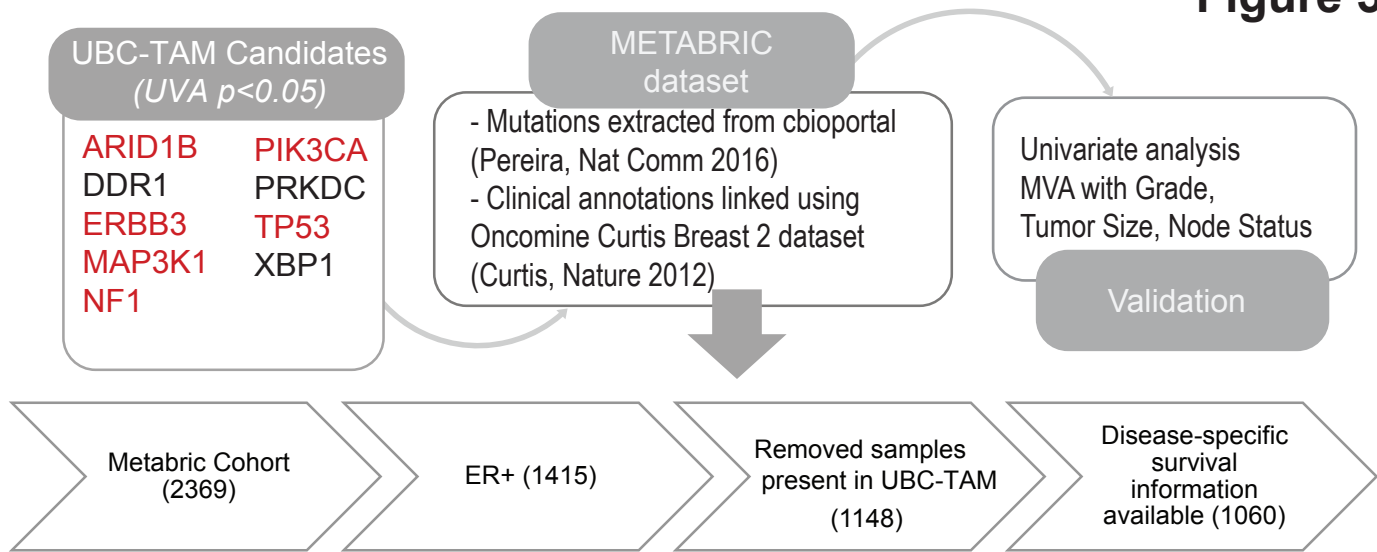
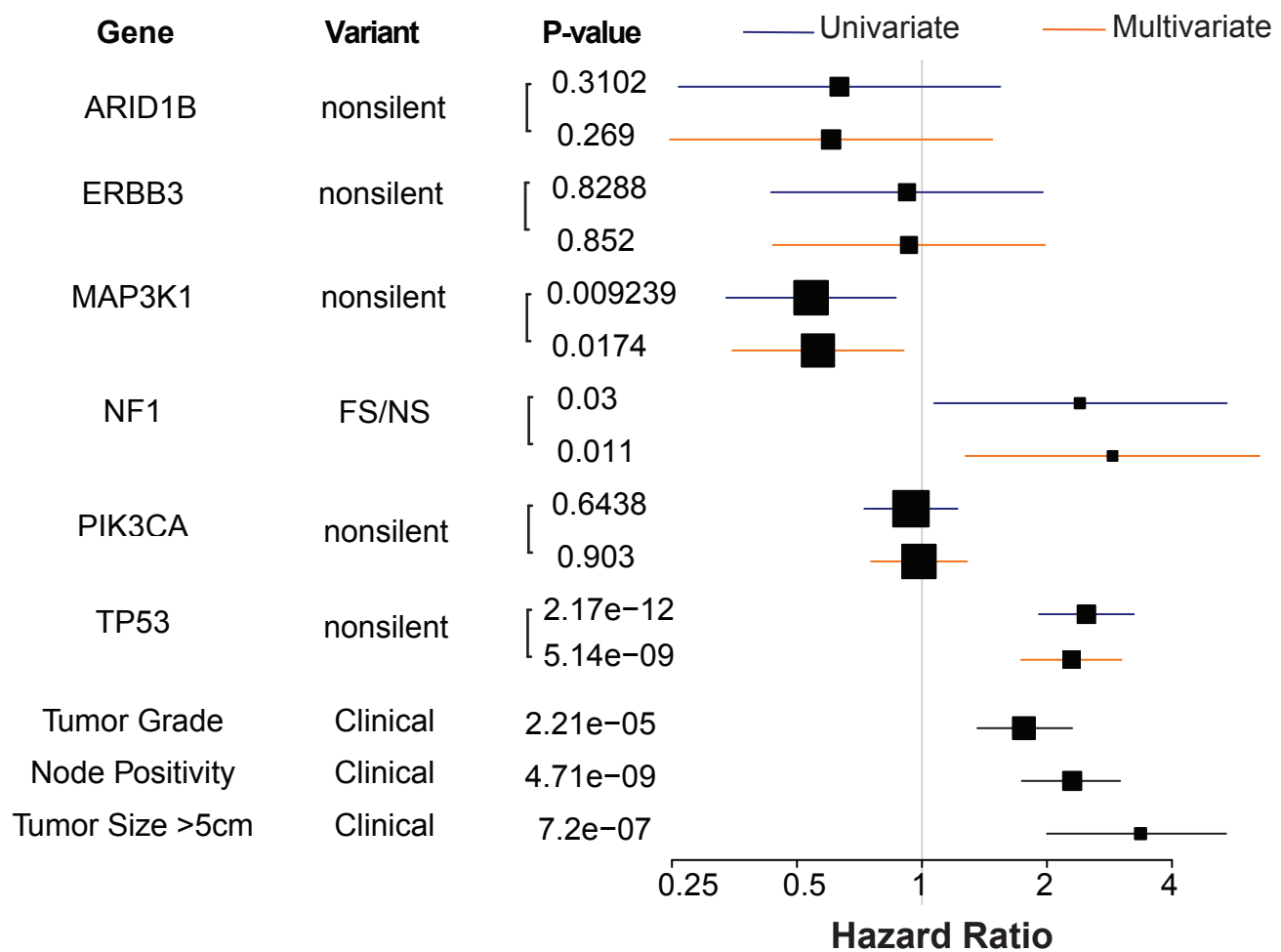
Figure 5.**a****b**

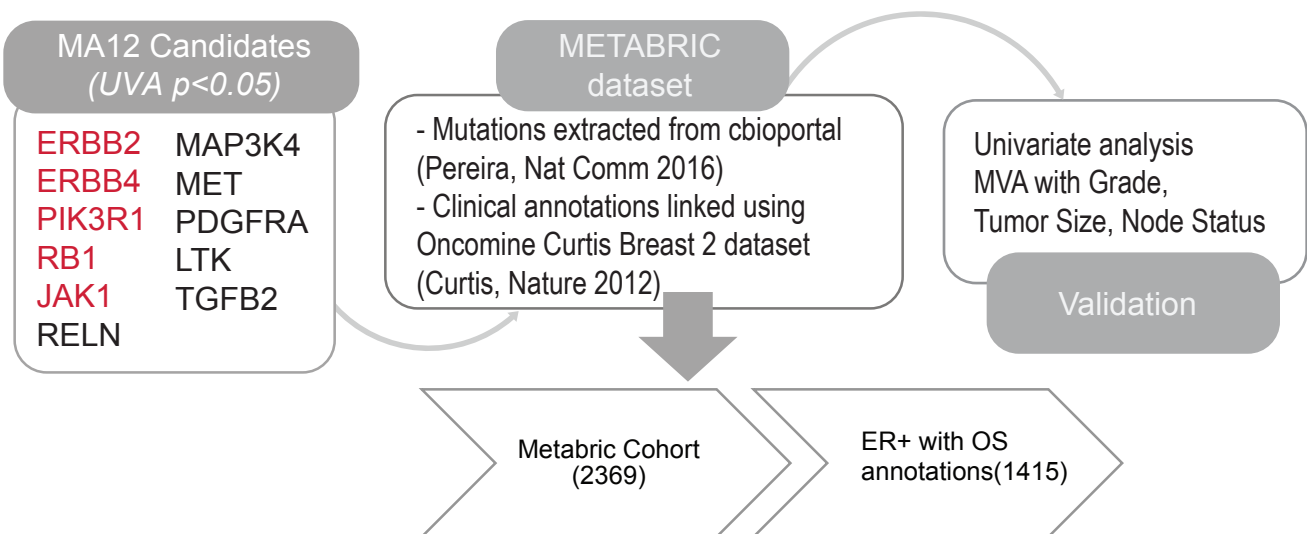
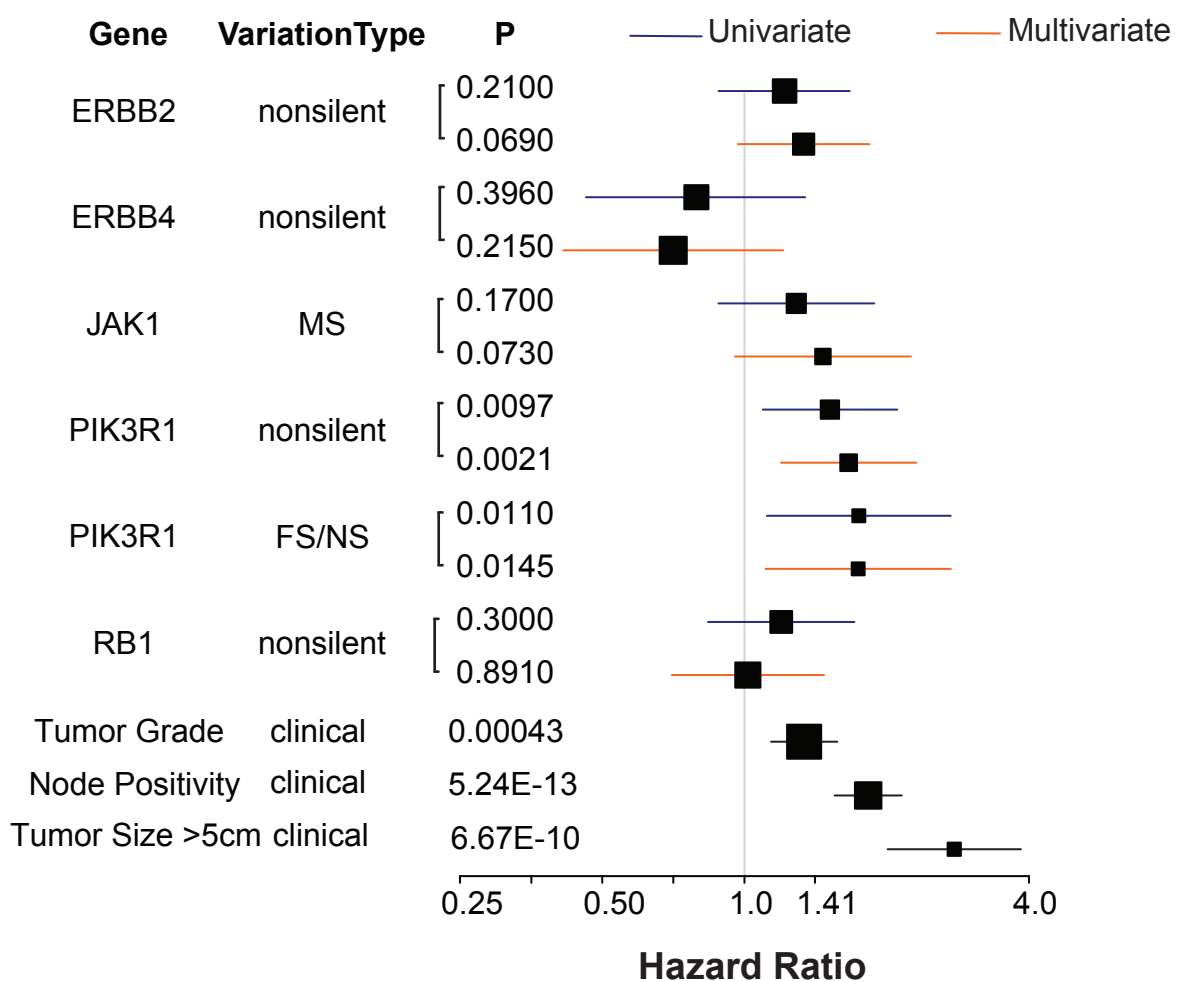
Figure 6.**a****b**

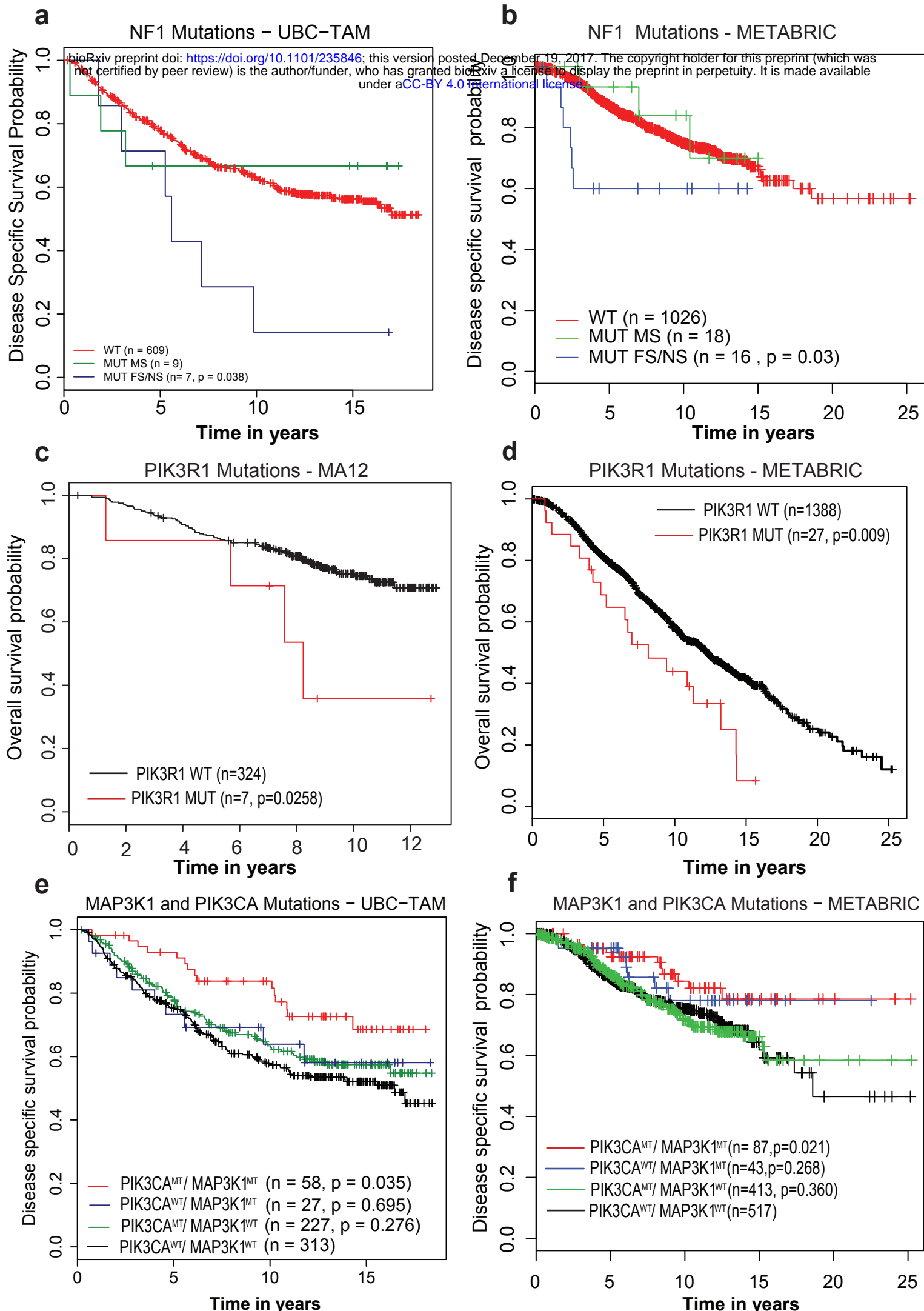
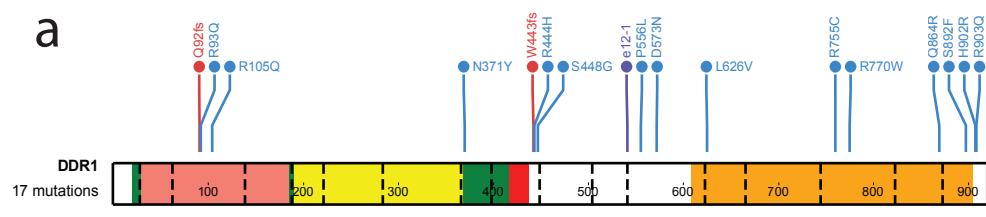
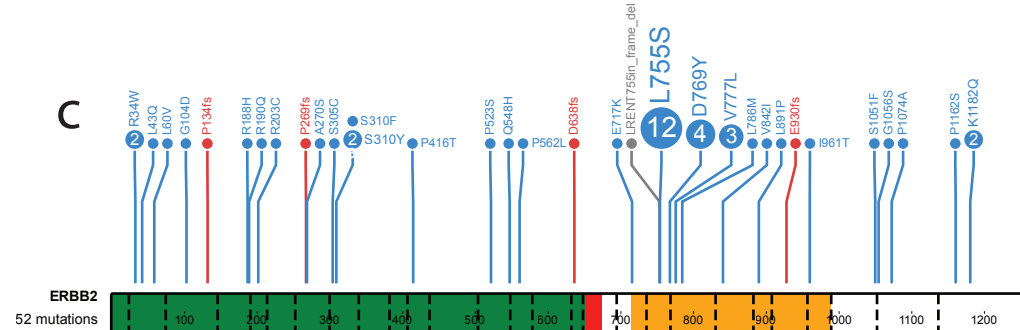
Figure 7.

Figure 8.

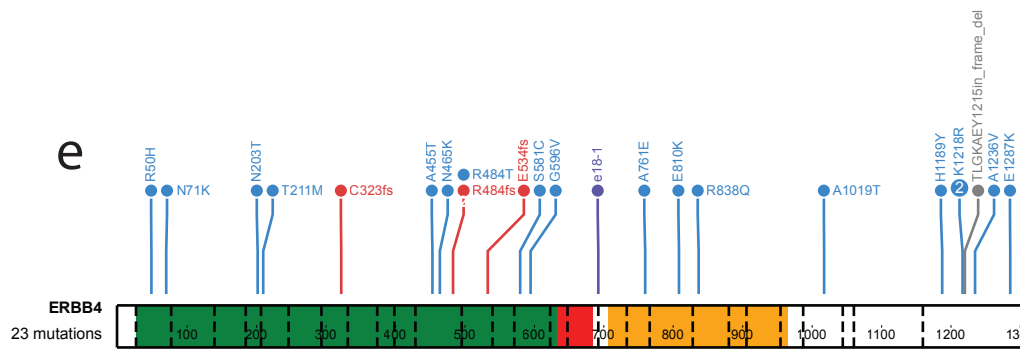
a



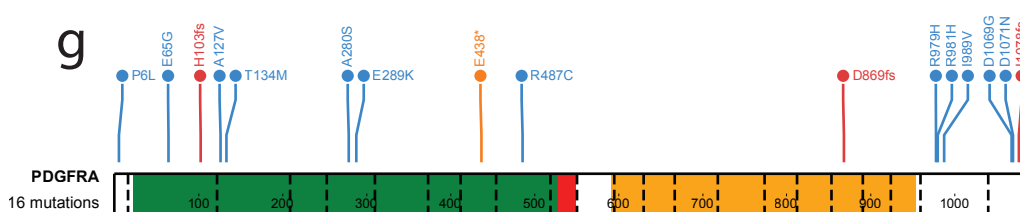
c



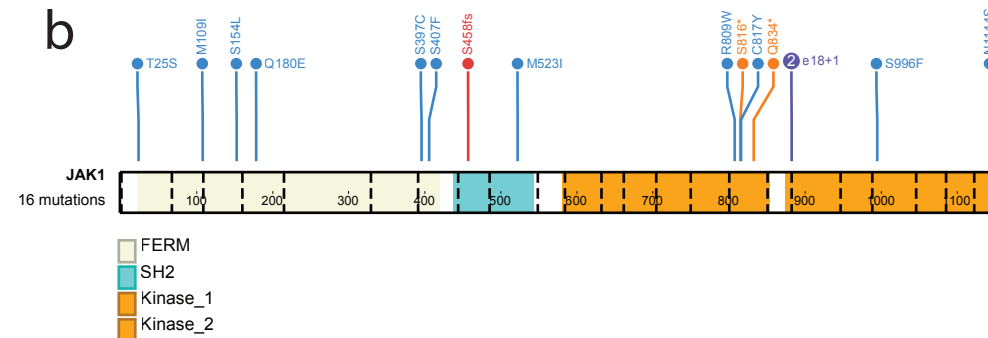
e



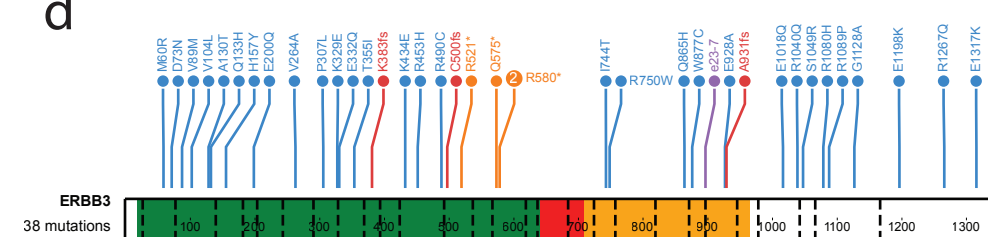
g



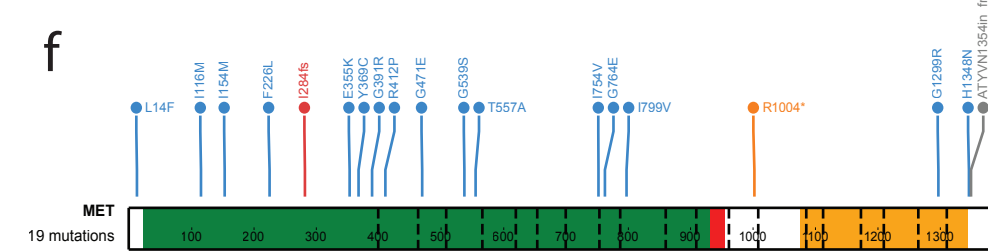
b



d



f



ECD

TM

Kinase

MISSENSE

FRAMESHIFT

PROTEINDEL

SPLICE

NONSENSE